On remote sensing of transient luminous events' parent lightning discharges by ELF/VLF wave measurements on board a satellite

F. Lefeuvre,[1] R. Marshall,[2] J. L. Pinçon,[1] U. S. Inan,[2] D. Lagoutte,[1] M. Parrot,[1] and J. J. Berthelier[3]

Received 11 February 2009; revised 2 April 2009; accepted 20 May 2009; published 11 September 2009.

[1] First recordings of satellite ELF/VLF waveform data associated with transient luminous event (TLE) observations are reported from the summer 2005 campaign coordinated by Stanford University and Laboratoire de Physique et Chimie de l'Environnement et de l'Espace (LPCE). TLEs are optically observed from the U.S. Langmuir Laboratory, while ELF/VLF waveform data are simultaneously recorded on board the Centre National d'Etudes Spatiales microsatellite DEMETER and on the ground at Langmuir. Analyses of ELF/VLF measurements associated with sprite events observed on 28 July 2005 and 3 August 2005 are presented. Conditions to trace back the wave emissions from the satellite to the source region of the parent lightning discharge are discussed. The main results concern: (1) the identification from a low Earth orbit satellite of the 0+ whistler signatures of the TLE causative lightning; (2) the identification of the propagation characteristics of proton whistlers triggered by the 0+ whistlers of the causative lightning, and the potential use of those characteristics; (3) recognition of the difficulty to observe sprite-produced ELF bursts in the presence of proton-whistlers; (4) the use of geographical displays of the average power received by the DEMETER electric field antennas over the U.S. Navy transmitter North West Cape (NWC) located in Western Australia to evaluate VLF transmission cones which explain the presence (28 July events) or the absence (3 August events) of propagation links between sferics observed at ground and 0+ whistlers observed on DEMETER; and (5) owing to electron-collisions, an optimum transfer of energy from the atmosphere to the ionosphere for waves with k vectors antiparallel, or quasi-antiparallel, to Earth's magnetic field direction.

Citation: Lefeuvre, F., R. Marshall, J. L. Pinçon, U. S. Inan, D. Lagoutte, M. Parrot, and J. J. Berthelier (2009), On remote sensing of transient luminous events' parent lightning discharges by ELF/VLF wave measurements on board a satellite, *J. Geophys. Res.*, *114*, A09303, doi:10.1029/2009JA014154.

1. Introduction

[2] Ground-based observations of ELF/VLF sferics have been extensively used for characterizing lightning discharges linked to transient luminous events (TLEs). Such measurements allow confirmation of sprite-causative cloud-to-ground (CG) flashes derived from lightning detection networks, characterization of the waveforms in terms of ELF slow-tail content [*Reising et al.*, 1996] and charge transfer [*Cummer et al.*, 1998] as well as identification of discharges not recorded by detection networks (either because they are not cloud-to-ground or because they are missed by the network criteria). Some of the results realized using ELF/VLF data include: connections between sprites and large positive lightning (+CG) strokes [*Boccippio et al.*, 1995], detection of unusual sprites triggered by negative lightning discharges [*Barrington-Leigh et al.*, 1999], and discovery of a large portion of −CG-initiated halos over the Central American region [*Frey et al.*, 2007]. Long time delays between TLEs and the nearest discharges observed by detection networks have resulted in the identification of clusters of sferics in association with early VLF changes and TLEs and their interpretation as signatures of in-cloud (IC) lightning flashes [*Johnson and Inan*, 2000; *Ohkubo et al.*, 2005; *Van der Velde et al.*, 2006; *Marshall et al.*, 2007]. In addition, comparisons with high-resolution photometer measurements have demonstrated the simultaneity of sprite luminosity and an ELF "second pulse" believed to be radiated by electrical currents within the heart of sprites [*Cummer et al.*, 1998].

[3] Largely owing to the lack of relevant waveform data, ELF/VLF remote sensing of TLE causative lightning discharges from space is much less developed. Although

[1]Laboratoire de Physique et Chimie de l'Environnement, Universite d'Orleans, CNRS, Orleans, France.
[2]Space, Telecommunications, and Radioscience Laboratory, Stanford, California, USA.
[3]Centre d'Etudes des Environnements Terrestre et Planétaires, IPSL, Université de Versailles et St Quentin-en-Yvelines, CNRS, Saint Maur, France.

0148-0227/09/2009JA014154

unravelling the transionospheric propagation of electromagnetic waves from a lighting discharge to a satellite may in some ways appear to be a more complicated inversion problem, it is clear that information collected above the source regions may usefully complement observations made below them. The propagation problem in hand can be briefly summarized as follows. Owing to reflections at the bottom of the ionosphere and at the ground, ELF and VLF energy originating in a lightning discharge propagates outward from the source region primarily in the Earth-ionosphere waveguide. As this guided propagation occurs with low attenuation rates [*Taylor and Sao*, 1970], these sferics can propagate over very long distances in the waveguide while a fraction of the wave energy may continually escape upward through the ionosphere. The main point to resolve is the process by which a wave generated in free space may cross the $X = f_{pe}^2/f^2 = 1$ plasma cutoff (where f_{pe} is the local plasma frequency and f is the wave frequency) to penetrate within the ionosphere, and the potential constraints it may impose for a maximum transfer of energy. Following *Helliwell* [1965], most authors consider that, because of the long wavelengths at ELF/VLF frequencies, the lower ionosphere may be assumed to have a sharp discontinuity in refractive index, so that implicitly the waves may not be affected by the plasma cutoff. However, that assumption may not be valid for wavelengths of the order or smaller than the thickness of the bottom layers.

[4] While lightning-generated wave energy propagating in the Earth-ionosphere waveguide is generally referred to as radio atmospherics (or sferics), upon transionospheric penetration to the overlying magnetosphere the signal is said to become a 0+ whistler [*Smith and Angerami*, 1968]. In this context, the notation of 0+ (zero-hop plus) signifies the fact that the signal has reached the satellite over a short-direct upward path, without having (yet) completed a magnetospheric hop. Upon crossing the geomagnetic equator the signal becomes a 1- (i.e., just short of completing its first hop), while upon reflection in the conjugate hemisphere the signal is now a 1+ (i.e., 1-hop plus). In satellite data, 0+ whistler signal components that are below ~1.8 kHz must have either entered the magnetosphere nearly overhead the causative discharge (in those cases where the satellite pass happens to be immediately overhead the thunderstorm) or necessarily propagated in the Earth-ionosphere waveguide in the quasi-transverse electromagnetic (QTEM) mode, since other modes (quasi-transverse electric or quasi-transverse magnetic) cannot propagate to long distances below this lowest mode cutoff frequency of ~1.8 kHz [see *Cummer*, 1997, and references therein]. The QTEM mode, on the other hand, suffers from increasing attenuation losses with increasing frequency so that in most cases 0+ whistler energy visible on a satellite in low Earth orbit exhibits significant energy only below ~1.2 to ~1.5 kHz. Observations of nonattenuated 0+ whistlers above the waveguide cutoff frequency of ~1.8 kHz, imply that waves have propagated in the Earth-ionosphere waveguide in QTE or QTM modes.

[5] To our knowledge, the first recording of satellite ELF/VLF waveform data associated with TLE observations was obtained during the summer 2005 coordinated campaign run by Stanford University and Laboratoire de Physique et Chimie de l'Environnement (LPCE). During that campaign, TLEs were observed on the ground from Langmuir Laboratory in New Mexico, and ELF/VLF waveform data were simultaneously recorded on board the CNES DEMETER microsatellite [*Parrot*, 2006] and at Langmuir and Palmer, Antarctica stations. Owing to the transient nature of the phenomena and the relatively short passages of the spacecraft over the ground-based observation region, very few well coordinated observations could be realized. The best example is from 28 July 2005 around 0502:45 UT where the distance between Langmuir and the foot of the magnetic line of force crossed by DEMETER was ~150 km [*Lefeuvre et al.*, 2006]. It is the objective of the present paper to present the results of a detailed analysis of these data: first, to point out relationships between ground-based and satellite-based measurements, and second, to contribute to the establishment of observational constraints for the French TARANIS CNES microsatellite project dedicated to the study of impulsive (or transient) transfers of energy between the atmosphere and the space environment [*Blanc et al.*, 2007; *Lefeuvre et al.*, 2008].

2. Instrumentation

[6] Ground-based observations were systematically performed during the nighttime periods of the summer 2005 campaign. TLEs were detected with a low-light camera system deployed at Langmuir (33° 9 N, 107°2 W) at ~3200 m altitude. Photometer data at 25 kS/s were recorded to remove any timing ambiguity. ELF/VLF measurements were performed by receivers located both at Langmuir and at Palmer station in Antarctica (64°77 S, 64°0 W). At each station two large triangular magnetic loop antennas are used to measure the N-S and E-W components in the band ~350 Hz to 45 kHz. The analog outputs of the two channels are sampled at 100 kS/s. For the optical as well as for the wave instruments, the timing is provided by GPS with 100 ns accuracy. The locations of causative lightning strokes are determined to an accuracy of ±0.5 km by the U.S. National Lightning Detection Network [*Cummins et al.*, 1998].

[7] ELF/VLF measurements in space were provided by the French DEMETER microsatellite [*Parrot*, 2006] launched at the end of June 2004. The satellite has a circular Sun-synchronous polar orbit at an altitude of 710 km. Nighttime passes over Langmuir were around 2230 MLT. The electric and magnetic wavefield components were measured by the *Berthelier et al.* [2006] electric field experiment (ICE) and the *Parrot et al.* [2006] magnetic field experiment (IMSC), respectively. In the ELF band ($\leq$1 kHz) the waveforms of the three electric and magnetic components were sampled at 2.5 kHz, which allows estimation of full propagation characteristics. In the VLF range ($\leq$17 kHz) waveforms of one electric and one magnetic component were sampled at 40 kHz.

[8] DEMETER has two main modes of operation: a burst mode, which provides waveform data and which is triggered when the satellite is above given seismic zones and other specific zones of interest like New Mexico; and a survey mode, which provides averaged power spectra.

[9] Since comparisons between ground-based and satellite-based data are only possible when the burst mode is on, it is only that mode which is considered here. According to the

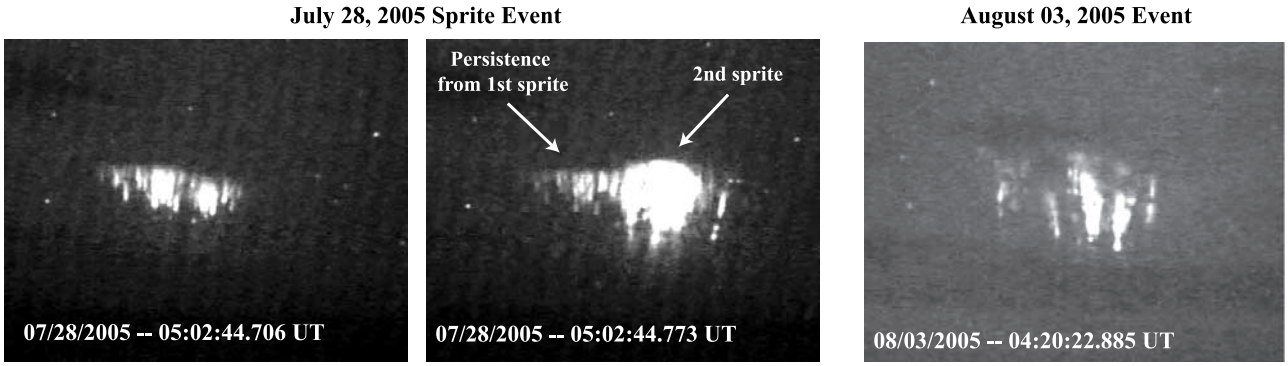

Figure 1. Sprite observations during the Langmuir-DEMETER campaign.

initial scientific objectives the uncertainty in the DEMETER timing is of the order of 10 ms which obviously limits comparisons.

3. Description of Data and Results

[10] During the summer 2005 campaign, three sets of TLEs were observed for DEMETER passes, in the burst mode, over the Langmuir station (see Figure 1). Two of them were recorded by the Langmuir photometers and cameras on 28 July (~0502:44 UT). The third was recorded on 3 August (~0420:22 UT). We will concentrate on the 28 July events.

[11] The 28 July and 3 August half-orbits are displayed in Figure 2. They are represented in red and blue. In both cases the satellite was on a south-to-north path. The location of the Langmuir station is indicated by an asterisk. The red and blue squares indicate the foot of the line of force crossed by Demeter at the time of the TLEs observations.

3.1. Sprite Observations

[12] The first sprite observation (Sprite 1) occurred at 0502:44.678 UT. It was observed at an azimuth of 202° (south-southwest). Examination of the NLDN data shows that a 75.2 kA +CG lightning flash at 27°863 N, 260°062 E occurred at 0502:44.671 UT, i.e., 7 ms before the sprite, in an azimuth (206°) consistent with the sprite observation. Assuming that the time delay between the causative +CG and the sprite is generally less than 20 ms, this +CG is most likely the parent lightning flash for Sprite 1. The estimated distance between Langmuir and the parent lightning flash is ~730 km. As a first approximation one may consider that the geographical coordinates of Sprite 1 are those of the parent lightning flash. However, an uncertainty of the order of 50 km may need be taken into account [*Wescott et al.*,

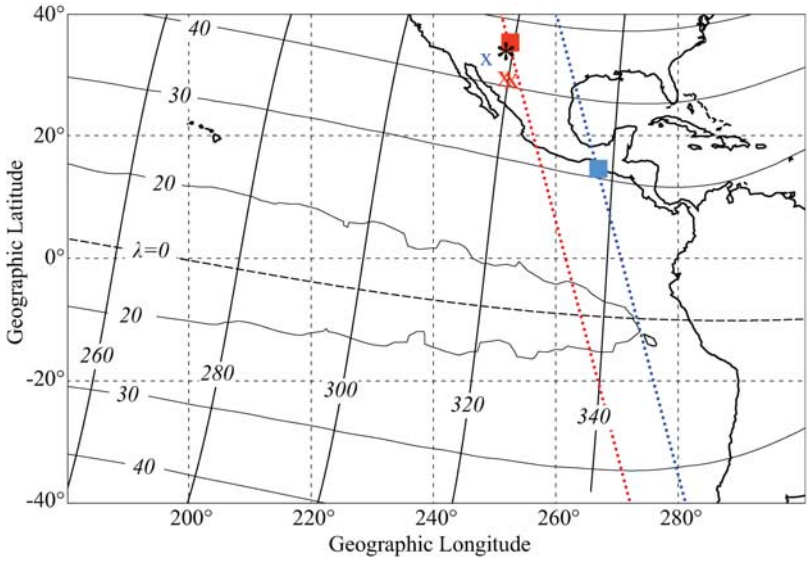

Figure 2. Geographical and invariant coordinates of the 28 July and 3 August 2005 observations. The asterisk indicates the location of the Langmuir Laboratory in New Mexico. The colored squares indicate the feet of the lines of force crossed by DEMETER at the time of the TLE observations. Crosses give the locations of the causative lightning flashes detected by the U.S. NLDN system. The 28 July orbit and the geographical coordinates for the parent lightning of TLE 1 and TLE 2 (27°86 N, 250°06 E; 27°97 N, 249°97 E) and the DEMETER location (34°98 N, 253°40 E) are given in red. The 3 August orbit and the geographical coordinates for the lightning of the TLE (32°10 N, 247°45 E) and the DEMETER location (12°59 N, 266°97) are given in blue.

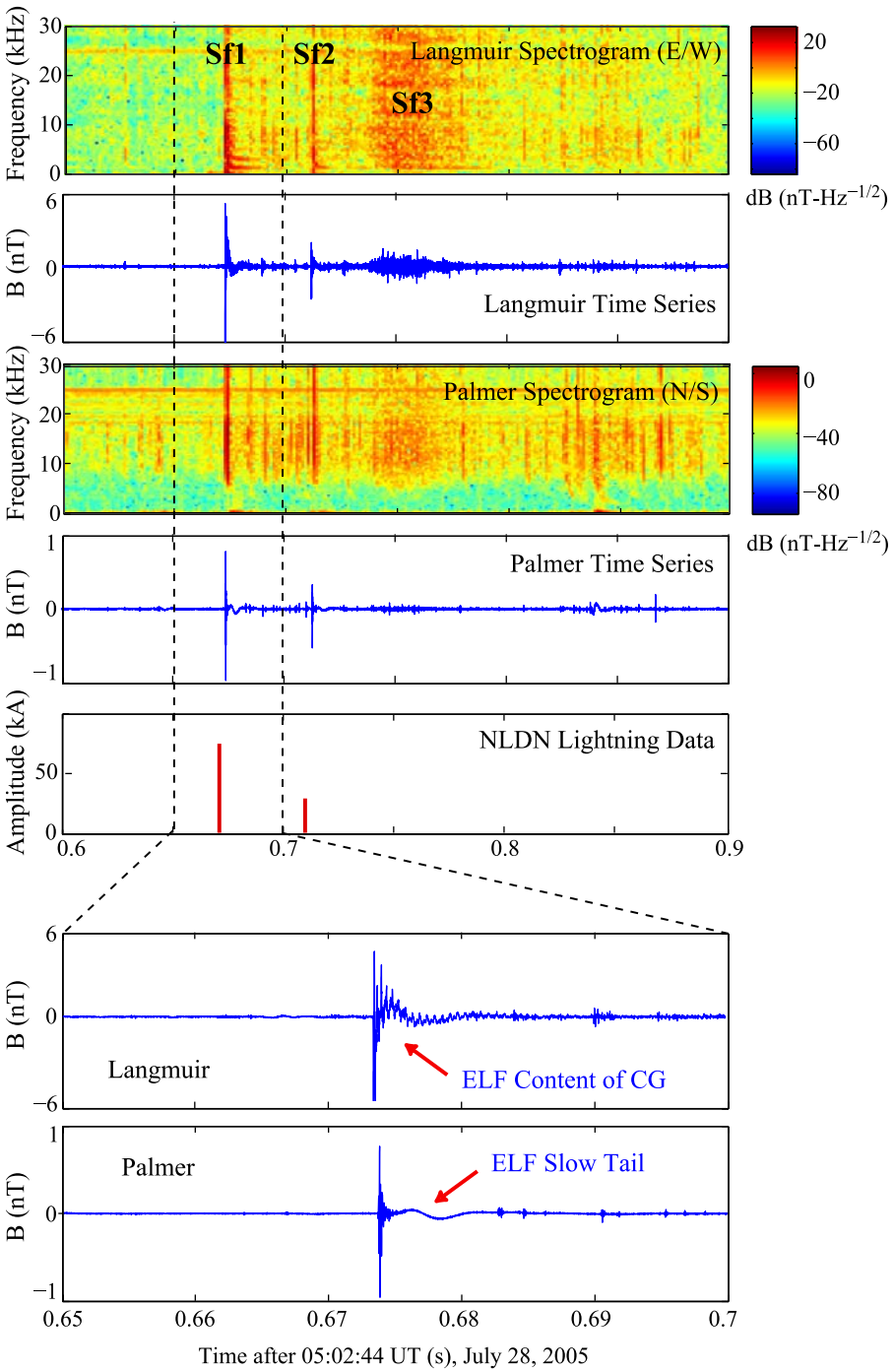

Figure 3. VLF/ELF ground-based measurements on 28 July 2005 around 0502:44 UT. Sferic 1 is observed at 0502:44.671 UT, sferic 2 at 0502:44.709 UT, and sferic 3 is in fact a cluster of sferics starting around 0502:44.740 UT.

2001; *São Sabbas et al.*, 2003]. It will not be considered here.

[13] The second sprite (Sprite 2) occurred at 0502:44.750 UT. It was observed at an azimuth of 206°. The closest lightning found in the NLDN data is a 28.9 kA +CG lighting flash, in a 207.3° azimuth, located at 27°974 N, 249°966 E and observed at 0502:44.709 UT. However, the peak current is rather low and the time delay is unusually long (41 ms). We return to this point later on with the analysis of the ELF/VLF data.

[14] The geographical and invariant coordinates of the parent lightning flashes and of the foot of the line of force crossed by DEMETER at the time of the TLEs observations are represented (in red) in Figure 2.

3.2. Ground-Based ELF/VLF Measurements

[15] Results of the analyses of the ELF/VLF signals (0–50 kHz) received at Langmuir and Palmer stations at the time of the sprite observations are displayed in Figure 3. From top to bottom: panels 1 and 2 show the ELF/VLF

spectrogram in the 0.35–30 kHz band and waveform data recorded at Langmuir; panels 3 and 4 show the ELF/VLF spectrogram and wave data recorded at Palmer; panel 5 shows NLDN lightning data; panels 6 and 7 show zoomed-in views of the Langmuir and Palmer waveform data at the time of observation of sprite 1. The time delay between the Langmuir and Palmer data is ~34 ms, consistent with the propagation time within the Earth-ionosphere waveguide, at a group speed which is approximately equal to the speed of light in free space. The amplitude of the signal received at Palmer is ~10 times smaller than at Langmuir. The lack of substantial attenuation below 1.8 kHz on the Langmuir spectrogram may mean that the signal propagated directly upward without substantial lateral propagation in the waveguide, consistent with the distance (~850 km) between satellite footprint and the lightning discharge. The attenuation below ~5 kHz on the Palmer signal is attributed to the fact that the dominant signal at these distances may be the QTM_2 mode, which exhibits a cutoff frequency of ~4 kHz.

[16] Three main events are observed on the Langmuir ELF/VLF spectrogram. The first event occurs at 0502:44.671 UT, i.e., at the time of the parent lightning of sprite 1; it is denoted sferic 1. The second event is a sferic associated with the lightning observed at 0502:44.709 UT, denoted sferic 2. The third event (sferic 3) is in fact a cluster of sferics which starts at 0502:44.740 UT. A frequency zoom shows that the sferic cluster has a lower-frequency cutoff around 1.6 KHz, i.e., it do not propagate in the waveguide QTEM mode. The three events are also detected at Palmer. Zoomed-in views (panels 6 and 7) of the ELF waveform data of sferic 1 (panels 2 and 4) show the signature of the ELF content of the CG at Langmuir and an ELF slow tail at Palmer. The strong ELF slow-tail is a signature of the continuing current which is required for a large charge moment change, thought to be a requirement for sprite production [*Cummer and Inan*, 2000].

[17] As already pointed out by *Ohkubo et al.* [2005] and *Van der Velde et al.* [2006], the presence of a sferic cluster a few tens of ms (here 41 ms) after the second +CG stroke suggests in-cloud (IC) lightning activity associated with that second discharge detected at 0502:44.709 UT by NLDN (see NLDN lightning data in Figure 3). Such IC activity may have triggered Sprite 2 through continuing currents, which may be signified by the multiplicity of in-cloud flashes producing the sferic burst.

3.3. DEMETER ELF/VLF Data

[18] DEMETER ELF/VLF data have been analyzed on the same time interval as in Figure 3. VLF spectrograms of single electric and magnetic wavefield components (E_x and B_y in the satellite frame of reference) are displayed in Figure 4. The most intense events, detected on the electric as well as the magnetic antennas, are 0+ whistlers for the two first events and a cluster of 0+ whistlers for the third event. Considering the UT arrival time at 20 kHz, and taking into account the time uncertainty on DEMETER (~10 ms), we conclude that the first 0+ whistler is sferic 1 after the transionospheric propagation, the second is sferic 2 after propagation, and the cluster of 0+ whistlers is the same cluster of sferics observed on the ground, after propagation through the ionosphere. The corresponding UT times are given in the legend of Figure 4. The distance between the DEMETER magnetic footprint and Langmuir is ~130 km. As a first approximation, comparing the maxima of the spectrograms derived from the magnetic measurements at Langmuir (36 nT^2/Hz) and on board DEMETER (10^{-5} nT^2/Hz) one finds a ratio of ~3.6 10^6, i.e., 65 dB in power.

3.4. Proton Whistlers

[19] Results of the spectral analysis of the DEMETER ELF data are displayed in Figure 5. The top panel exhibits upgoing proton whistlers produced by upgoing 0^+ whistlers at the altitude of the proton crossover frequency f_{cr} (here $f_{cr} \sim 380$ Hz), where a polarization reversal may occur [*Gurnett et al.*, 1965]. The proton whistlers have a resonance at the local proton gyrofrequency f_H^+ (here $f_H^+ \sim 500$ Hz). The succession of proton whistlers produces an emission band at f_H^+. According to its power density, it would be surprising that sprite-produced ELF bursts, generated at the sprite altitude, and observed at ground, would be visible on the DEMETER ELF spectrogram. The most intense proton whistlers, produced by the ELF part of the first 0+ whistler, present two very scarce characteristics according to *Stefant* [1985]: (1) there is no frequency gap between f_{cr} and f_H^+(generally the gap extends slightly above f_H^+) on the "electron whistler" part, and (2) the "electron whistler," which is observed here on the magnetic as well as the electric components (the magnetic component is shown in Figure 5), is electromagnetic over the entire frequency band even around f_H^+. This strongly suggests that there are clearly one electron and one proton mode without unknown energy transfers between f_{cr} and f_H^+. Owing to the time resolution, the proton whistler produced by the ELF part of the second 0+ whistler cannot be dissociated from the first one.

[20] Propagation characteristics of the proton whistlers have been derived from the waveforms of the three magnetic field components. Using the *Lefeuvre et al.* [1986] analysis techniques one finds (1) the absolute value of cos θ, where $\theta = (\boldsymbol{k}, \mathbf{B}_o)$ is the polar angle made by the wave normal direction $\boldsymbol{k}$ with the direction of Earth's magnetic field, and (2) the sense of polarization. The results are displayed in the bottom panel of Figure 5. Denoting the propagation angle derived from the analysis techniques as ψ, one has $\theta = \psi$ for $\psi < 90°$ and $\theta = \pi - \psi$ for $\psi > 90°$. One observes three features: first, that the distinction between the right-hand polarized "electron whistler" (in red) and the left-hand polarized "proton whistler" (in green) is better seen in this analysis than it is on the spectrogram; second, that the "electron whistler" does not disappear between f_{cr} and f_H^+; and third, that the polar angles have estimated values of the order of 30° in the two modes. Very weak time stationarities do not allow more accurate estimations.

[21] A review of the propagation characteristics of the waves at the vicinity of the crossover frequency has been provided by *Budden* [1985]. At the altitude of the proton crossover frequency the only electron whistler waves which can pass through are those with a wave normal direction **k** near a critical coupling cone centered on $\theta = 0°$. More precise values are predicted by the *Wang* [1971] full-wave model which shows that for incident waves with θ values below 10°, all the wave energy stays in the electron whistler mode, whereas for the range $10° < \theta < 30°$, the percentage

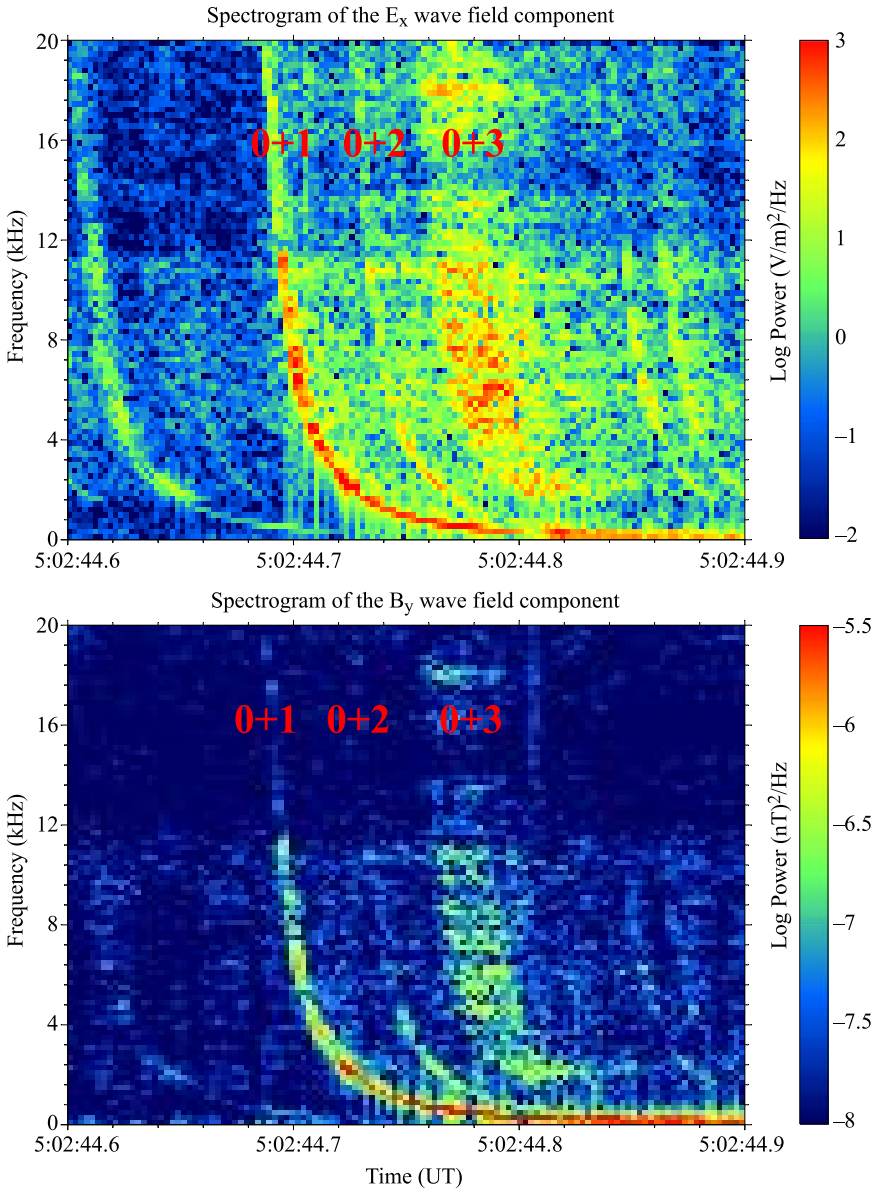

Figure 4. DEMETER VLF measurements on 28 July 2005 around 0502:44 UT. The most intense 0+ whistlers simultaneously observed on the spectrogram of (top) E_x electric field component and (bottom) B_y magnetic field component are at 0502:44.685 UT and 0502:44.723 UT and start at 0502:44.753 UT for a cluster of 0+ whistlers. There is an uncertainty on the DEMETER UT time of the order of 10 ms.

of wave energy in the right-hand mode drops from 90% to 10%. Experimental confirmations of these estimates are provided by *Chan et al.* [1972]. All those characteristics are consistent with the results displayed in Figure 5.

[22] Although further statistical studies are needed, the above analyses suggest (1) that 0+ whistlers associated with sprite-producing lightning propagate toward high altitudes with $\boldsymbol{k}$ vectors parallel or nearly parallel to the Earth magnetic field (which does not mean that the waves are ducted), so that raypaths may be traced back from a satellite to the ionosphere entry points; and (2) that, according to their group velocity at the vicinity of the resonance, the proton whistlers generated by successive 0+ whistlers merge and so that, around the local proton gyrofrequency, and in a larger frequency domain at higher receiver sensitivity, limited potential signatures of sprite current pulses may be masked by proton whistlers.

4. Discussion

[23] A full feasibility study of remote sensing of TLE-causative lightning discharges, from ELF/VLF measurements on board a satellite, requires solving the "direct problem"; i.e., understanding how the electromagnetic radiation associated with a lightning discharge propagates up to the satellite altitude. This is an old problem, with still several important open questions. The objective of section 4 is to take advantage of the data presented in section 3 to point out a number of useful guidelines.

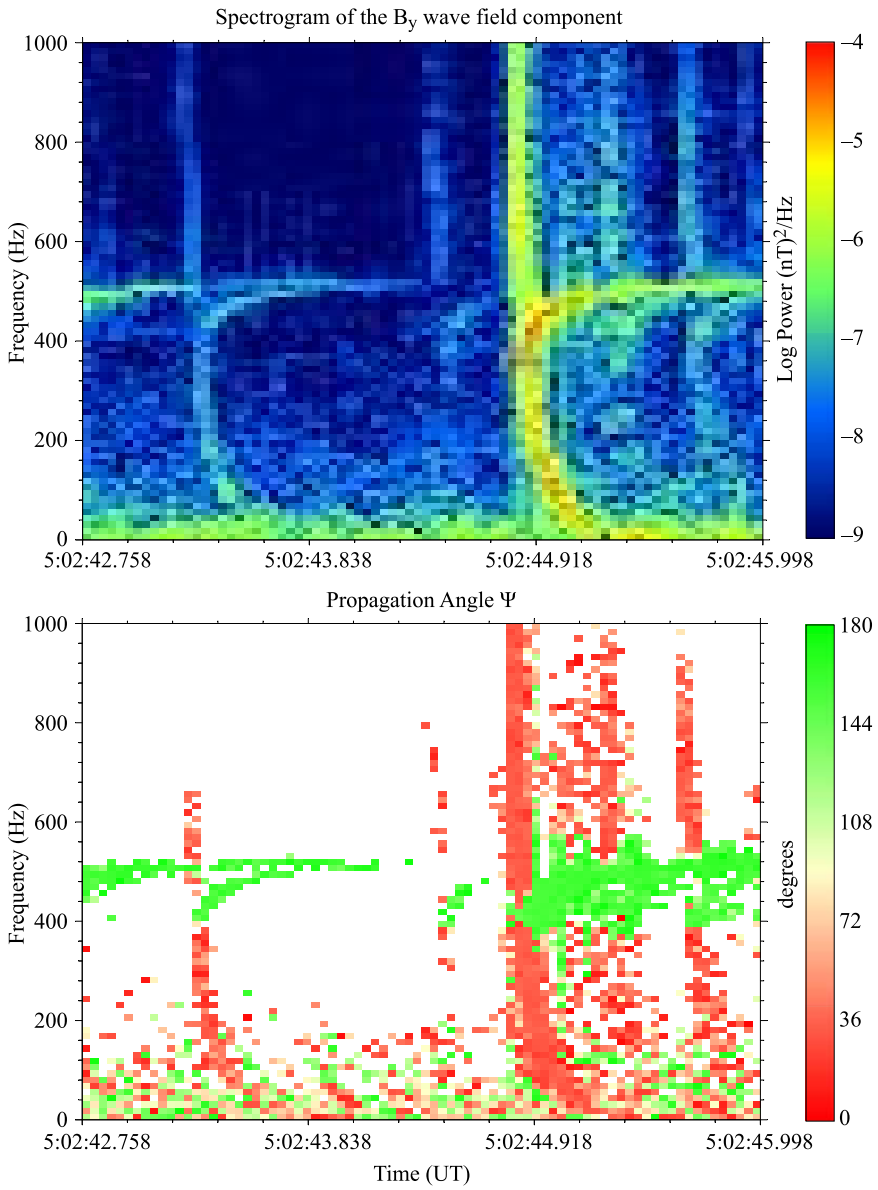

Figure 5. Wave analysis for the DEMETER ELF data on 28 July 2005 around 0502:44 UT. (top) Spectrogram of the B_x field component and (bottom) propagation mode and ψ values. For $\psi < 90°$, $\theta = \psi$, whereas for $\psi > 90°$, $\theta = \pi - \psi$.

4.1. Evaluation of Transmission Cones

[24] We turn our attention to the sprite event observed on 3 August 2005. The parent lightning of the sprite observed at 0420:22.839 UT was located at 32°10 N and 247°45 E. The foot of the line of force crossed by DEMETER a few ms later was at 12°59 N, 266°97 E (see Figure 2), at a distance of ~3060 km. The frequency/time structures of the sferics seen at the Langmuir station do not present prominent features such as those of the 28 July events (see Figure 3), and so are more difficult to compare; however, spectral analyses of the Langmuir and DEMETER data over the relevant time intervals (the spectrograms are not represented here) have been undertaken, but do not show any clear link. This lack of correlation raises the question of the size of the transmission cone (or of the multiple transmission cones in case of multiple entry points) in the upper part of the ionosphere. Although extrapolations of these results may not be obvious, we propose to examine that question by referring to DEMETER observations of ground-based VLF transmitters.

[25] A common characteristic of the VLF transmitter data acquired on DEMETER is the strong attenuation of the signal around the geomagnetic equator. The attenuation is a function of the power of the transmitter and of the proximity to the geomagnetic equator. As a first approximation, one may consider that a rather "dead zone" exists for the VLF transmitter data at ±15° around the geomagnetic equator. However, the 3 August TLE event occurred slightly before the DEMETER entry into that "dead zone" (although being at 12°59′ geographic latitude, the satellite is 22° above the geomagnetic equator), and so it is difficult to claim that it is the proximity to the geomagnetic equator that may explain the absence of propagation links between the sferics observed at

Langmuir and the 0+ whistlers observed on DEMETER. In such a case we must also consider transmission cones.

[26] A geographical display of the average power received by the electric field antennas over the U.S. Navy transmitter North West Cape (NWC) (19.8 kHz, 1 MW radiated power, 21.82° S, 114.17° E) located in Western Australia (see *Sauvaud et al.* [2008] and Figure 6) provides a good opportunity to evaluate a transmission cone. According to its power, the transmitter is observable over the latitude range from 60° S to 60° N, including the equatorial regions. However, there are well defined peaks just above the transmitter location (obviously the strongest) and at the conjugate point. Above the transmitter location the maximum value of the power density is $10^{4.7}$ $\mu V^2/(m^2.Hz)$. The width of the power peak at a hundredth of this maximum is of the order of ±10° in latitude and ±15° in longitude. At lower power densities (approximately a thousandth of the maximum) the contour of the average power received above the NWC is more complex. A detailed interpretation of that low power density contour is not obvious and probably not pertinent. The average power received on DEMETER has been estimated by averaging data from September 2005 to December 2006. During that period, numerous geomagnetic storms were observed, including two strong (Kp = 7) and one severe (Kp = 8) storm (see NOAA Space Weather Scales: http://www.swpc.noaa.gov/NOAAscales/). The effects of those geomagnetic storms on the density gradients, and of the sensitivity of the propagation characteristic parameters to those density gradients [*James*, 1972], result in a statistical broadening of the zone of reception of the NWC signal at the altitude of DEMETER. Biases in the geographical distributions are unavoidable. The fringes, pointed out by numerous space experimenters, are generally interpreted in terms of interferences produced by transmitted waveguide modes [*Aubry*, 1967; *Cerisier and James*, 1970]. Such waveguide interference does not affect the sferics considered here since, as already mentioned, sferics without lower cutoff frequencies below ∼1.8 kHz propagate in the QTEM mode only.

[27] As a result, we consider that lightning flashes have transmission cones of the order of ±10 to 15° in latitude and longitude. Similar values may be derived from the transmission cones of other VLF transmitters [*Clilverd et al.*, 2008]. As discussed above, the transmission cones may be reduced at the vicinity of the geomagnetic equator.

[28] As a consequence, it is clear that DEMETER crosses the transmission cones of the parent lightning flashes of the two 28 July TLEs (as seen in Figure 2, the distances between the parent lightning flashes and the foot of the line of force are Δlat = 7°12, Δlong = 3°34; Δlat = 7°01, and Δlong = 3°43, respectively) whereas it does not cross the transmission cone of the 3 August event (Δlat = 19°50, Δlong = 13°97).

[29] Many more coordinated ground based and satellite based measurements are needed to develop reliable transmission cone models, taking into account the spectral power densities as well as of the geographical and geophysical conditions.

4.2. Wave Propagation at the Entry of the Lower Layers of the Ionosphere

[30] An important point to be examined for developing a transmission cone model, and hence for checking the hypotheses to be used for remote sensing of lighting discharges from satellite observations of 0+ whistlers, is the process of wave propagation at the entry point of the lower layers of the ionosphere. In particular, the altitude at which the wave frequency becomes equal to the local electron plasma frequency f_{pe}, i.e., at the crossing of the $X = f_{pe}^2/f^2 = 1$ plasma cutoff, is of great importance. Considerable insight may be found in the analysis of the 28 July events.

[31] The model generally used to explain the escape or leakage of wave energy through the lower boundary of the ionosphere in the ELF/VLF frequency range is the *Helliwell* [1965] sharp-density model. It is considered that, owing to the very sharp increase in the electron density (three orders of magnitude) over an altitude range of a few km (which, as shown later on, is not always true), the wave energy which penetrates upward necessarily ends up with a nearly vertical wave $\boldsymbol{k}$ vector direction. In addition, substantial absorption losses occur as the wave energy traverses the highly collisional regions of ∼70–90 km altitude, where the imaginary part of the refractive index exhibits a maximum. In that model the ELF/VLF waves cross the X = 1 plasma cutoff without being affected by it.

[32] However, the density variation with height is not always very sharp. This is the case when using the IRI 2001 model, run for the wave and plasma parameters of 28 July 2005 at 0500 UT and for geographic latitudes and longitudes of 30° and 250°, respectively. The derived f_{pe} profile is represented in Figure 7. This results in an E layer thickness on the order of 50 km, followed by a valley of approximately the same size between the E and F layers. In such a case, we observe that (1) below the X = 1 plasma cutoff, the rotation of the $\boldsymbol{k}$ vector toward the vertical direction is limited and does not prevent the existence of $\boldsymbol{k}$ **vec**tors along Earth's magnetic field direction at X = 1, and (2) VLF waves are affected by the X = 1 plasma cutoff and are constrained by conditions taken into account in the *Ellis* [1956] and *Budden* [1985] radio-window model. It is likely that the inclusion of a D layer, known to be difficult to measure and to model [*Bilitza*, 2001], would provide even softer gradients and thus softer rotations of the $\boldsymbol{k}$ vectors below X = 1.

[33] The radio-window model is based on the variation with X of the square of the refractive index (n^2) for a cold electron plasma. The square of the refractive index depends on: X, $Y = f_{ce}/f$ (with f_{ce} the local electron gyrofrequency), the θ angle with respect to $\mathbf{B}_0$, and a complex value noted $U = 1 - iZ$ in which $Z = \nu/2\pi f$ and ν is the electron collision frequency. In the presence of collision the refractive index is given by the Appleton-Lassen formula:

$$n^2 = 1 - \frac{A(X)}{B(X, Y, \theta) \pm C(X, Y, \theta)} \tag{1}$$

with

$$A(X) = X(U - X)$$

$$B(X, Y, \theta) = U(U - X) - \frac{Y_T^2}{2}$$

$$C(X, Y, \theta) = \left(\frac{Y_T^4}{4} + Y_L^2(1 - X^2)\right)^{1/2}$$

and

$$Y_T = Y \sin\theta$$

$$Y_L = Y \cos\theta$$

[34] In order to define the radio-window concept, let us first consider a collisionless plasma, i.e., to take U = 1. For Y $\sim$ 100, which corresponds to values one may expect for VLF waves at the bottom of the ionosphere (at 60 km, f_{ce} is of the order of 1.4 MHz). The variation of n^2 as a function of X is given in Figure 8. Red curves are for $\theta = 0°$ and blue curves for $\theta = 10°$. The pluses and dots represent the n^2 solutions with the plus and minus signs in the denominator of the second term of (1), respectively; these are typically labeled ordinary and extraordinary waves, respectively [*Helliwell*, 1965; *Budden*, 1985]. Clearly, the passage from free space (X $\sim$ 0) to the ionosphere (X > 1) is only possible for waves with $\theta = 0°$ at X = 1. Under these conditions, the dispersion relations of the extraordinary and ordinary modes take the same value. The longitudinal extraordinary mode couples with the longitudinal ordinary mode, known as the whistler (W) mode. The whistler mode is the only mode which may propagate up to the satellite altitude and above. Such is not the case for the ordinary longitudinal waves that couple with the extraordinary longitudinal mode before reaching the X = 1 + Y reflection level. That reflection level is generally reached a few tens of kilometers above X = 1. In the case of a cold collisionless plasma, all upgoing oblique waves are reflected back to the ground.

[35] Coming back to Figure 8, it is interesting to note that access to the resonance of the whistler mode is only possible when upgoing whistler mode waves cross a plasma region decreasing X values. According to the profile of Figure 7, this is only possible when waves with frequencies between $\sim$250 and 400 kHz cross the valley between the *E* and *F* layers. In such a case, pure longitudinal waves propagate upward whereas oblique waves have access to the resonance as soon as they leave the *E* layer (i.e., as soon as they cross the X = 1 plasma cutoff a second time). Accurate models of *D* and *E* layers should allow the potential deposit of wave energy at $\sim$100 km altitude and possibly lower.

[36] According to *Budden* [1985], when collisions are taken into account, wave energy is transferred through the X = 1 cutoff for wave normal vectors in a small cone of angles around $\theta = 0°$. Quantitative information may be obtained by using the electron profile of Figure 7 and the *Wait and Spies* [1962] electron-collision profile $\nu = 1.816 \times 10^{11} \exp\{-0.15h\}$ where *h* is the altitude. The variations in *h* of the real and imaginary parts of the refractive index are given in Figure 9 (f = 10 kHz), for θ values of 0°, 20°, 40° and 60°. One observes that if there are no zero or/and infinite values in the real part of the refractive index at the altitude of the X = 1 plasma cutoff, there are strong decreases in the imaginary parts, i.e., strong absorption. For the frequencies considered here, the level of absorption strongly depends on the values of the θ angle. It is small from $\theta = 0°$ to 20° then rapidly increases with the θ values. The effect is more pronounced for f = 50 kHz than for f = 10 kHz, but decreases again above $\sim$150 kHz. From $\sim$250 Hz, the effect of the collision frequency becomes negligible: 0 and infinite values appear in the real part of the refractive index around the X = 1 plasma cutoffs, and absorption disappears.

[37] The important result of the above simulation is that, due both to the propagation mode coupling at the X = 1 plasma cutoff and to the electron collisions, the transmission of wave energy from the atmosphere to the ionosphere is made through a complex ***k***-filtering system. The transfer function of this system depends on the geographical coordinates of the parent lightning, the density profile at the bottom of ionosphere (in particular the *D* and *E* regions), the electron-collision profile, and the wave frequency. This ***k***-filtering is detrimental to the wave energy conveyed by oblique ***k*** vectors, and instead the wave energy transmitted is mainly conveyed by longitudinal and quasi-longitudinal waves. The effect is stronger at HF and VHF frequencies than at VLF frequencies and obviously at ELF frequencies. However, it cannot be neglected for the development of lightning transmission cone models. Obviously, ray-tracing performed at the altitude where the ***k***-filtering system operates is invalid. The existence or lack of ionospheric and/or magnetospheric ducts above those altitudes is not discussed here, although these must be taken into account for a full treatment.

[38] Several observations seem to be consistent with the existence of a ***k***-filtering system at the bottom of ionosphere. The analyses of the 28 July 2005 events, with a perfect correspondence between the sferics detected at Langmuir and the 0+ whistlers seen on DEMETER (Figures 3 and 4), and quasi-longitudinal ***k*** vectors in the electron part of the DEMETER proton whistlers (Figure 5), correspond with (1) the generation of lightning discharges well away of the DEMETER magnetic foot print ($\sim$850 km southwest), (2) entry points of the associated sferics approximately above Langmuir ($\sim$130 km south of the DEMETER magnetic foot print), and (3) propagation nearly along the line of force from the entry point to the altitude of DEMETER. In the same way, the ***k***-filtering system concept could be used to explain satellite observations of well-defined transmission cones above VLF transmitters (e.g., Figure 6) and more specifically displacements poleward or equatorward of the observed peak wave power according to the geographical coordinates of the VLF transmitters [*Clilverd et al.*, 2008].

[39] With regard to the latter point, it may be interesting to recall the *Budden* [1985] latitudinal condition for a wave energy transmission to the ionosphere and the magnetosphere. It is:

$$Y > 0.5\left(1 + l_Z^{-2}\right)$$

where l_z is the direction cosine of the axis of the refractive index surface. That condition is not very restrictive for the VLF part of the upgoing 0+ whistlers. As an example, writing α as the angle made by the vertical with Earth's magnetic field and assuming f_c = 1.4 MHz at the bottom of the ionosphere, one observes that waves around 1 kHz cross the ionosphere up to $\alpha \sim 85°$ whereas waves around 50 kHz cross the ionosphere up to $\alpha \sim 80°$. This is consistent with the above discussion of the attenuation of the VLF transmitter data in the equatorial regions. As a consequence, except for a narrow domain around the magnetic equator,

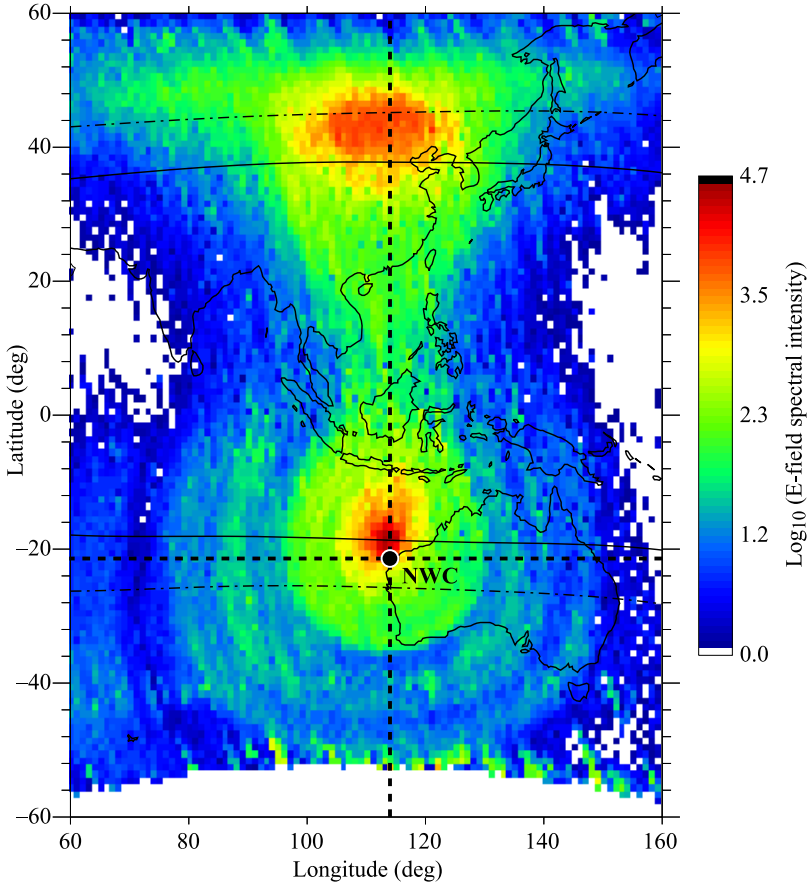

Figure 6. Geographic display of the average power received by the electric field antennas over the U.S. Navy transmitter North West Cape, Australia (NWC) [*Sauvaud et al.*, 2008].

most lightning induced 0+ whistlers can indeed reach the satellite.

5. Summary

[40] ELF/VLF wavefields, simultaneously observed at the Langmuir Laboratory ground-based station and on board the DEMETER satellite, at the time of the detection of sprite events by a camera deployed at the Langmuir station, have been fully analyzed. These lead to the following results.

[41] For the two 28 July events:

[42] 1. Despite a ~900 km distance between the parent lightning discharges and the DEMETER magnetic footprint, but in agreement with the ~130 km distance between Langmuir and the DEMETER foot print, a clear propagation link exists between the ELF/VLF sferics observed at the Langmuir station (sferic 1, sferic 2, then a cluster of sferics) and the ELF/VLF 0+ whistlers observed on board DEMETER.

[43] 2. We observe a 65 dB difference between the power spectral densities of the sferics received at ground and the 0+ whistlers received on DEMETER.

[44] 3. We observe proton whistlers, with a clear electromagnetic "electron whistler" part (without a frequency gap), triggered by the 0+ whistlers of the sprite causative lightning discharges.

[45] 4. Propagation characteristics of the proton whistlers are analyzed which confirm the proton whistler model and suggest quasi-longitudinal propagations from the bottom of the ionosphere to the satellite altitude.

[46] 5. We find power spectral densities of the proton whistlers at the proton gyrofrequency which may mask sprite-produced ELF bursts.

[47] For the 3 August event, as one could expect according to the ~3060 km distance between the parent lightning and the DEMETER magnetic footprint, and the ~2850 km distance between Langmuir and the DEMETER magnetic foot print, no propagation link is found between the sferics recorded at ground and the 0+ whistlers recorded on board the satellite.

[48] In order to explain the presence of propagation links of the sferics and 0+ whistlers observed on 28 July 2005 and the absence of any link on 3 August 2005, transmission cones of lightning flashes have been evaluated from the average power spectral density observed by DEMETER electric field antennas over the U.S. Navy transmitter NWC located in Western Australia [*Sauvaud et al.*, 2008]. Taking the width of the peak at a hundredth of its maximum, and assuming that the power spectral densities of the 0+ whistlers are weaker than the spectral density of the NWC signal observed on DEMETER, one may consider that the lightning transmission cones are of the order of ±10 to 15° in latitude and longitude at the satellite altitude. Because of the attenuation of the VLF signals around the geomagnetic equator, the sizes of these cones may be reduced within the equatorial regions. It has been shown that those estimates

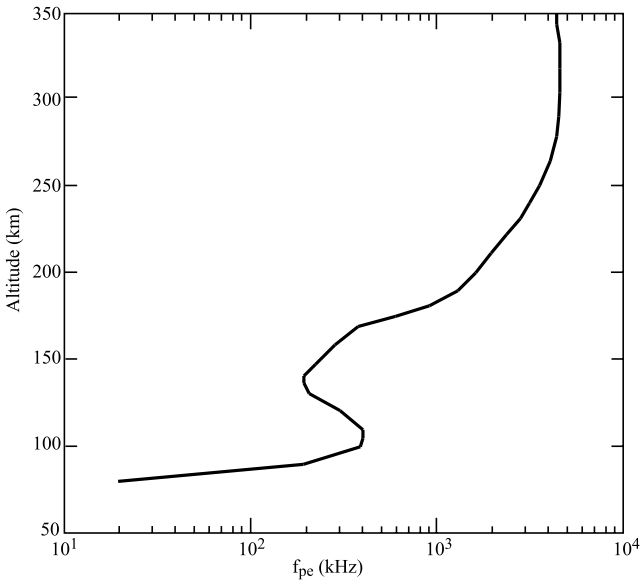

Figure 7. Plot of the IRI 2001 model for 28 July 2005 at 0500 UT for geographic latitude and longitude of 32° and 253°.

are in agreement with the analyses of the 28 July 2005 and August 2005 events.

[49] Simulations performed using the IRI 2001 model of the ionospheric density profile at the time and geographical location of the 28 July event and the *Wait and Spies* [1962] electron-collision profile, have shown that the transmission of wave energy from the atmosphere to the ionosphere is made through a complex ***k***-filtering system, the transfer function of which depends on the density profile at the bottom of ionosphere (in particular the *D* and *E* regions), the electron-collision profile, and the wave frequency. The wave energy transmitted is mainly conveyed by longitudinal or quasi-longitudinal waves. The effect is stronger at HF and VHF frequencies than at VLF frequencies and obviously at ELF frequencies. However, it cannot be neglected for the development of lightning transmission cone models. The existence of such a ***k***-filtering system is consistent with the simultaneous observations at Langmuir and on board DEMETER for the 28 July 2005 event (the station is located close to the satellite magnetic foot print and the propagation is quasi-transverse at the satellite altitude). Moreover, it can explain preferable transfers of wave energy at specific entry points to the ionosphere such as those pointed out by *Clilverd et al.* [2008] for ground-based VLF transmitters. In addition, these simulations shows that for density profiles with a valley between the *E* and *F* layers (see Figure 7), waves of frequencies *f* between the minimum plasma frequency of the valley and the maximum plasma frequency of the *E* layer (here $f \sim 250$ kHz) may have access to the resonance, i.e., may deposit wave energy at the upper boundary of the *E* layer. Similar phenomena could be expected at the upper boundaries of *D* layers.

[50] These results demonstrate that, provided the transfer function of the ***k***-filtering system be modeled, ELF/VLF remote sensing of the signatures of parent lightning discharges that lead to TLEs and/or TGFs is feasible. This technique may be used in the absence of ground-based

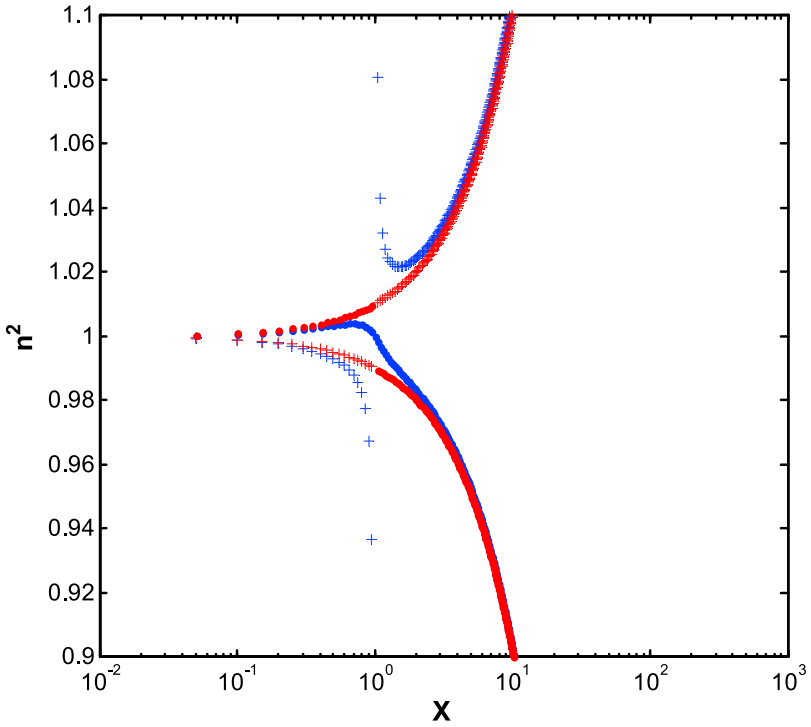

Figure 8. Dependence of n^2 on X for a cold collisionless electron plasma when Y = 100. Red curves are for $\theta = 0°$, and blue curves are for $\theta = 10°$. The n^2 solutions are derived from the Appleton-Lassen formula. Pluses and dots refer to the positive and negative signs in the denominator of the second term, respectively.

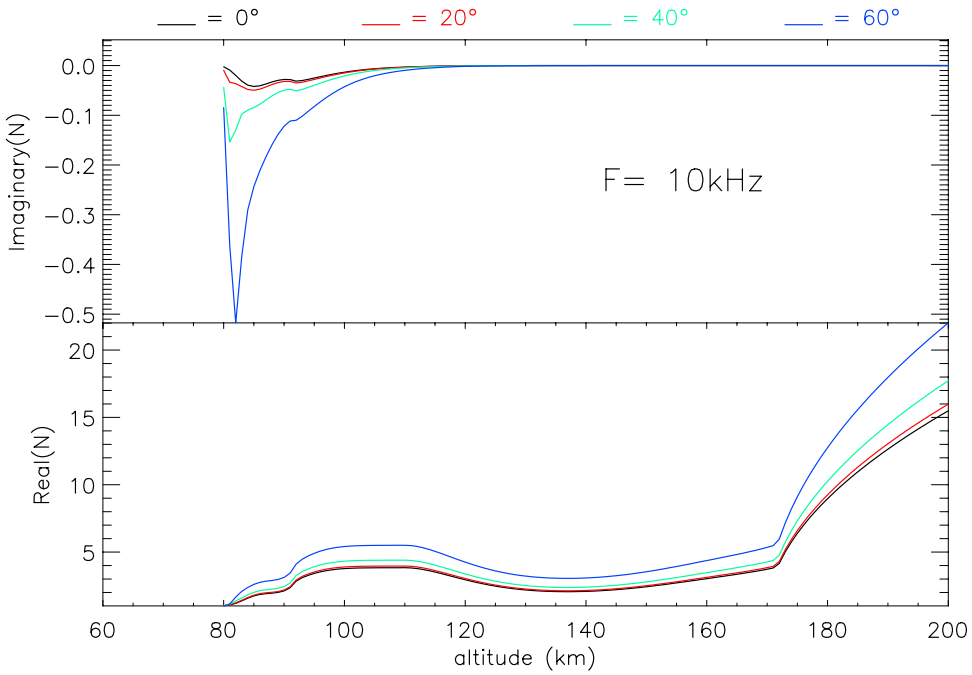

Figure 9. Variation of n^2 with altitude h for $f = 10$ kHz. The electron plasma frequency profile is that of Figure 7. The electron collision frequency profile is given by $\nu = 1.816 \times 10^{11} \exp\{-0.15h\}$. Calculations are made for $\theta = 0°$, 20°, 40°, and 60°.

stations and/or in case of timing problems between the satellite and the ground-based station. However, to fully assess this capability it is necessary to use a larger data set of comparisons between ground-based and satellite-based measurements to experimentally characterize the ELF/VLF transmission cones crossed by low-altitude satellites.

[51] As pointed out in the discussion on proton whistlers, spectral properties of 0+ whistlers may be used to facilitate the inverse ray tracing. Signals observed alone above the crossover frequency or those with little or no frequency gaps with proton whistlers probably propagate largely along Earth's magnetic field. This is consistent with the fact that the refractive index surface for whistler mode waves for $Y \ll 1$ dictates group velocity directions (i.e., ray directions) along Earth's magnetic field for a limited range of $\boldsymbol{k}$ vector angles. Numerous other observations are needed to determine whether proton whistlers are often associated with TLE parent lightning flashes observed from Earth. However, such a result would be entirely expected, especially for observations immediately overhead the active thunderstorm, since the resulting intensity of the proton whistlers must necessarily be proportional to the intensity of the 0+ electron whistler components that arrive at the region of the crossover frequency. In this context, it should be noted that significant wave energy content at the frequencies of the proton whistlers (i.e., <500 Hz) would only escape through the ionosphere near the source, since such frequencies are strongly attenuated in the Earth-ionosphere waveguide.

[52] An important conclusion for identification of events from low Earth orbit satellites, and in particular for the upcoming TARANIS mission, is that it will be important to forecast joint optical and ELF/VLF measurement campaigns with ground-based stations, and it is imperative to embark on wave experiments allowing (1) systematic detection of 0+ whistlers (triggered proton whistlers included), and (2) an extended observation band of up to a few hundred kHz where collisions may be neglected and where deposition of wave energy at the bottom of the E and D layers may be observed.

[53] **Acknowledgments.** The Stanford component of this work was supported by the U.S. Office of Naval Research grant N00014-03-1-033. Robert Marshall is supported by a Stanford Lieberman Fellowship. The LPCE component was supported by the Centre National d'Etudes Spatiales. The space data are based on observations with the ICE and IMSC instruments embarked on DEMETER. The authors wish to thank Ken Cummins and John Cramer of Vaisala, Incorporated, for access to NLDN data and SPDF/Modelweb for access to the IRI ionospheric models.

[54] The editor thanks H. Gordon James and another reviewer for their assistance in evaluating this paper.

References

Aubry, M. P. (1967), Influence des gradients horizontaux de densité électronique sur la direction des normales d'ondes TBF dans l'ionosphère, *Ann. Geophys.*, *23*(4), 467–476.

Barrington-Leigh, C. P., U. S. Inan, M. Stanley, and S. A. Cummer (1999), Sprites triggered by negative lightning discharges, *Geophys. Res. Lett.*, *26*, 3605–3608, doi:10.1029/1999GL010692.

Berthelier, J. J., et al. (2006), ICE, the electric field experiment on DEMETER, *Planet. Space Sci.*, *54*, 456–471, doi:10.1016/j.pss.2005.10.016.

Bilitza, D. (2001), International Reference Ionosphere 2000, *Radio Sci.*, *36*, 261–275, doi:10.1029/2000RS002432.

Blanc, E., F. Lefeuvre, R. Roussel-Dupré, and J. A. Sauvaud (2007), TARANIS: A microsatellite project dedicated to the study of impulsive transfers of energy between the Earth atmosphere, the ionosphere and the magnetosphere, *Adv. Space Res.*, *40*, 1268–1275, doi:10.1016/j.asr.2007.06.037.

Boccippio, D. J., E. R. Williams, S. J. Heckman, W. A. Lyons, I. T. Baker, and R. Boldi (1995), Sprites, ELF transients, and positive ground strokes, *Science*, *269*(5227), 1088–1091, doi:10.1126/science.269.5227.1088.

Budden, K. G. (1985), *The Propagation of Radio Waves*, Cambridge Univ. Press, New York.

Cerisier, J. C., and H. G. James (1970), Etude du satellite FR-1 de la propagation d'ondes très basse fréquence dans l'ionosphère à basse latitude, *Ann. Geophys.*, *26*(4), 829–843.

Chan, K. W., R. K. Burton, R. Holze, and E. Smith (1972), Measurement of the wave-normal vector of proton whistler on OGO 6, *J. Geophys. Res.*, *77*, 635–639, doi:10.1029/JA077i004p00635.

Clilverd, M. A., C. J. Rodger, R. Gamble, N. P. Meredith, M. Parrot, J.-J. Berthelier, and N. R. Thomson (2008), Ground-based transmitter signals observed from space: Ducted or nonducted?, *J. Geophys. Res.*, *113*, A04211, doi:10.1029/2007JA012602.

Cummer, S. A. (1997), Lightning and ionosphere remote sensing using VLF/ELF radio atmospherics, Ph.D. thesis, Stanford Univ., Stanford, Calif.

Cummer, S. A., and U. S. Inan (2000), Modeling ELF radio atmospheric propagation and extracting lightning currents from ELF observations, *Radio Sci.*, *35*, 385–304.

Cummer, S. A., U. S. Inan, T. F. Bell, and C. P. Barrington-Leight (1998), ELF radiation produced by electrical currents in sprites, *Geophys. Res. Lett.*, *25*, 1281–1284.

Cummins, K. L., M. J. Murphy, E. A. Bardo, W. L. Hiscox, R. B. Pyle, and A. E. Pifer (1998), A Combined TOA/MDF Technology Upgrade of the U.S. National Lightning Detection Network, *J. Geophys. Res.*, *103*, 9035–9044.

Ellis, G. R. (1956), The Z propagation hole in the ionosphere, *J. Atmos. Terr. Phys.*, *8*, 243.

Frey, H. U., et al. (2007), Halos generated by negative cloud-to-ground lightning, *Geophys. Res. Lett.*, *34*, L18801, doi:10.1029/2007GL030908.

Gurnett, D. A., S. D. Shawhan, N. M. Brice, and R. L. Smith (1965), Ion cyclotron whistlers, *J. Geophys. Res.*, *70*, 1665–1688, doi:10.1029/JZ070i007p01665.

Helliwell, R. A. (1965), *Whistlers and Related Ionospheric Phenomena*, Stanford Univ. Press, Stanford, Calif.

James, H. G. (1972), Refraction of whistler-mode waves by large-scale gradients in the middle-latitude ionosphere, *Ann. Geophys.*, *28*(2), 301–339.

Johnson, M. P., and U. S. Inan (2000), Sferic clusters associated with early/Fast VLF events, *Geophys. Res. Lett.*, *27*, 1391–1394.

Lefeuvre, F., Y. Marouan, M. Parrot, and J. L. Rauch (1986), Rapid determination of the sense of polarization and propagation for random electromagnetic wave fields, Application to GEOS-1 and Aureol-3 data, *Annal. Geophys.*, *4*, 457–468. (Correction, *Annal. Geophys.*, *5*, 251–252.)

Lefeuvre, F., E. Blanc, R. Marshall, and M. Parrot (2006), The TARANIS project: On the on-board identification of sprites related EM emissions, *Eos Trans. AGU*, *87*(52), Fall Meet. Suppl., Abstract AE42A-04.

Lefeuvre, F., E. Blanc, R. Roussel-Dupré, J. A. Sauvaud, and J. L. Pinçon (2008), TARANIS—A micro-satellite project dedicated to the physics of TLEs and TGFs, *Space Sci. Rev.*, *137*, 301–315, doi:10.1007/s11214-008-9414-4.

Marshall, R. A., U. S. Inan, and W. A. Lyons (2007), Very low frequency sferic bursts, sprites, and their association with lightning activity, *J. Geophys. Res.*, *112*, D22105, doi:10.1029/2007JD008857.

Ohkubo, A., H. Fukunishi, Y. Takahashi, and T. Adachi (2005), ELF/VLF sferic evidence for in-cloud discharge activity producing sprites, *Geophys. Res. Lett.*, *32*, L04812, doi:10.1029/2004GL021943.

Parrot, M. (2006), Preface to the special issue of *Planetary and Space Science* "DEMETER," *Planet. Space Sci.*, *54*, 411–412, doi:10.1016/j.pss.2005.10.012.

Parrot, M., et al. (2006), The magnetic field experiment IMSC and its data processing on board DEMETER: Scientific objectives, description of the firs results, *Planet. Space Sci.*, *54*, 441–455, doi:10.1016/j.pss.2005.10.015.

Reising, S. C., U. S. Inan, T. F. Bell, and W. A. Lyons (1996), Evidence for continuing current in sprite-producing cloud-to-ground lightning, *Geophys. Res. Lett.*, *23*, 3639, doi:10.1029/96GL03480.

São Sabbas, F. T., D. D. Sentman, E. M. Wescott, O. Pinto Jr., O. Mendes Jr., and M. J. Taylor (2003), Statistical analysis of space-time relationships between sprites and lightning, *J. Atmos. Sol. Terr.*, *65*, 525, doi:10.1016/S1364-6826(02)00326-7.

Sauvaud, J. A., R. Maggiolo, C. Jacquey, M. Parrot, J. J. Berthelier, R. J. Gamble, and C. G. Rodger (2008), Radiation belt electron precipitation due to VLF transmitters: Satellite observations, *Geophys. Res. Lett.*, *35*, L09101, doi:10.1029/2008GL033194.

Smith, R. L., and J. J. Angerami (1968), Magnetospheric properties deduced from OGO 1 observations of ducted and nonducted whistlers, *J. Geophys. Res.*, *73*, 1–20, doi:10.1029/JA073i001p00001.

Stefant, R. J. (1985), Comments on the proton whistler generation process, *Planet. Space Sci.*, *33*, 333–349, doi:10.1016/0032-0633(85)90065-0.

Taylor, W. L., and K. Sao (1970), ELF attenuation rates and phase velocities observed from slow-tail components of atmospherics, *Radio Sci.*, *5*, 1453–1460, doi:10.1029/RS005i012p01453.

Van der Velde, A., A. Mika, S. Soula, C. Hadoulpis, T. Neubert, and U. S. Inan (2006), Observations of the relationship between sprite morphology and in-cloud lightning processes, *J. Geophys. Res.*, *111*, D15203, doi:10.1029/2005JD006879.

Wait, J. R., and K. P. Spies (1962), Characteristics of the Earth-ionosphere wave guide for VLF radio waves, *NBS Tech. Note U.S., 300*.

Wang, T.-I. (1971), Intermode Coupling at ion whistler frequencies in a stratified collisionless ionosphere, *J. Geophys. Res.*, *76*, 947–959, doi:10.1029/JA076i004p00947.

Wescott, E. M., H. C. Stenbaek-Nielsen, D. D. Sentman, M. J. Heavner, D. R. Moudry, and F. T. S. Sabbas (2001), Triangulation of sprites, associated halos and their possible relation to causative lightning and micrometeors, *J. Geophys. Res.*, *106*, 10,467–10,477.

J. J. Berthelier, Centre d'Etudes des Environnements Terrestre et Planétaires, IPSL, Université de Versailles et St Quentin-en-Yvelines, CNRS, 4 Avenue de Neptune, F-94107 Saint Maur, France.

U. S. Inan and R. Marshall, Space, Telecommunications, and Radioscience Laboratory, 350 Serra Mall, Packard Building, Stanford, CA 94305-9515, USA.

F. Lefeuvre, D. Lagoutte, M. Parrot, and J. L. Pinçon, Laboratoire de Physique et Chimie de l'Environnement, Universite d'Orleans, CNRS, F-45071 Orleans Cedex 2, France. (lefeuvre@cnrs-orleans.fr)